Original Article
Tyrosine kinase inhibitor sunitinib targets the vasculature of clear cell renal cell carcinoma: a morphometrical study of treatment effect

Lu Chen[1*], Longwen Chen[2,3*], Jie Huang[2,4], Danfeng Xu[1], Linhui Wang[1], Ming Zhou[2,5]

[1]Department of Urology, Second Military Medical University, Shanghai, China; [2]Department of Anatomic Pathology, Cleveland Clinic Foundation, Cleveland, OH, USA; [3]Laboratory Medicine and Pathology, Mayo Clinic, Scottsdale, AZ, USA; [4]Department of Pathology, Eastern Long Island Hospital, NY, USA; [5]Department of Urology and Pathology, New York University Langone Medical Center, NY, USA. *Equal contributors.

Abstract: Tyrosine kinase inhibitor sunitinib is thought to exert its anti-tumor effect by modulating angiogenesis in clear cell renal cell carcinoma (ccRCC). The pathological changes after sunitinib treatment have, however, rarely been studied in surgically resected ccRCC specimens. Such studies are important as they allow researchers to examine whether sunitinib targets the intended tissue and the effectiveness of treatment. We analyzed the pathological and immunohistochemical features of 14 surgically resected ccRCCs following sunitinib treatment and 25 untreated ccRCCs. Treated and untreated ccRCCs were similar in tumor size, nuclear grade and pathological stage. The treated tumors, however, showed significantly higher extent of tumor necrosis (32%) and more likely to have pericellular fibrosis (100%) and vasculopathy involving medium/large vessels (78.6%) compared with untreated tumors (23%, 20% and 40%, respectively, p<0.03). The treated tumors showed 47% reduction in microvessel density demonstrated on CD34 immunohistochemistry compared to the untreated tumors (64 vs 33, p=0.003). Architectural disruption, including vascular dilation and fragmentation, were significantly more common in treated tumors. VEGFR-2 expression (VEGFR-2/CD34 ratio) was higher on tumor microvessels in treated tumors than untreated tumors (0.95 vs 0.81, p=0.04). Our study confirms that tumor microvessels are the primary target of sunitinib treatment in ccRCCs. Sunitinib treatment significantly reduces the microvessel density and also produces significant structural disruption that lead to hypoxia, ischemia and necrosis in tumors. The treatment also increases the VEGFR-2 expression on the residual tumor microvessels and may contribute to the occurrence of resistance to sunitinib treatment.

Keywords: Clear cell renal cell carcinoma, tyrosine kinase Inhibitor, sunitinib, microvessel density, angiogenesis, VEGFR-2

Introduction

Clear cell renal cell carcinoma (ccRCC) accounts for about 70% of RCCs in adults. The carcinogenesis of ccRCC is related to von Hippel Landau (*VHL*) gene inactivation [1-3], although recent studies have also demonstratred the important role of chromatin remodeling genes and metabolic pathways [4-9]. Most sporadic ccRCCs show *VHL* gene inactivation by deletion, mutation, or promoter hypermethylation [3, 10]. It is clear that VHL protein plays a critical role in hypoxia inducible factor (HIF) homeostasis and regulation of genes in hypoxia inducible pathway. In ccRCC in which *VHL* gene expression is inactivated, HIF protein accumulates in the cytoplasm and subsequently diffuses into the nuclei to activate the genes regulated by HIF including vascular endothelial growth factor (VEGF), platelet derived growth factor (PDGF) and carbonic anhydrase IX (CAIX) [11, 12]. These growth factors bind to their corresponding receptors to activate cellular signaling cascades to promote cell proliferation, growth and survival. The unchecked stimulation of these pathways leads to tumor development, growth and progression. Overexpression of VEGF and PDGF is particularly relevant to clear
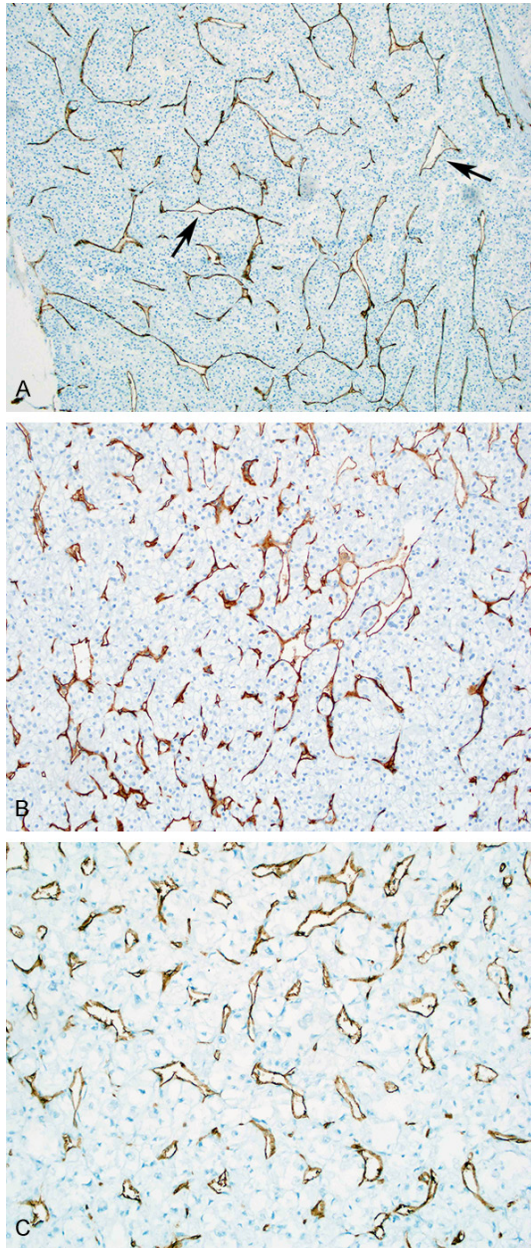
Figure 1. Morphology of microvessels in clear cell renal cell carcinoma. On CD34 immunostains, tumor microvessels form delicate and arborizing vasculature without conspicuous lumens (A). They, however, may become dilated (A, arrows) and discontinuous. Tumor microvessel dilatation is categorized as normal (A), focal (B) and diffuse (C) when <10%, 10-50% and >50% of microvessels show dilatation. Similarly tumor microvessel fragmentation is categorized as normal (A), focal (B) and diffuse (C) when short and discontinuous microvessels account for <10%, 10-50% and >50% of microvessels.

cell renal carcinogenesis as they are potent proangiogenic factors and promote tumor an-

giogenesis and therefore growth and progression.

20-30% of ccRCCs present with metastatic disease. After surgical resection, 1/3 of patients develop distant metastasis [3]. Treatment for advanced ccRCC remains a challenge. Many small molecular inhibitors have been developed to target genes implicated in the HIF regulated pathways. In recent years, sunitinib has been recommended as a first line therapy for metastatic ccRCC [13]. As a multi-kinase inhibitor, it selectively inhibits several tyrosine kinases, including vascular endothelial growth factor receptor 2 (VEGFR-2), platelet-derived growth factor receptor ß (PDGFR-ß), stem cell factor receptor (Kit) and Fms-related tyrosine kinase 3 (Flt-3). The antitumor effect of sunitinib is thought to be mediated by inhibition of three major pathways [10]. Inhibition of the Protein Kinase C (PKC) pathway causes rapid disruption of existing tumor blood vessels which leads to acute tumor regression. Inhibition of MAP kinase pathway inhibits new blood vessel formation which leads to tumor growth delay or slow tumor regression. Finally inhibition of PI3K pathway may have a direct effect on cancer cells causing cancer cell death.

Thought to primarily targeting tumor angiogenesis [14], the anti-tumor mechanism of sunitinib is not entirely clear. Most published studies used cell culture and animal xenograft models [14-16]. The pathologic and molecular changes after sunitinib treatment have been studied in ccRCC surgical resection specimens in only a few studies [17, 18]. None, however, provided detailed morophometric analysis of the treatment effect. Our current study was aimed to identify the histological changes in treated tumors and to explore the possible anti-tumor mechanism by studying the morphometric changes in tumor vasculature, expression of key molecules such as VEGFR-2 and CAIX after treatment.

Material and methods

Patient cohort

14 ccRCC tumors with neoadjuvant sunitinib treatment prior to surgical resection (study cases) and 25 ccRCC tumors with no treatment (control cases) were included. Study and control cases were matched for ISUP nucleolar

Table 1. Clinical and pathological features of clear cell renal cell carcinomas

Clinicopathological features	Untreated	Treated	P value
No. patients	25	14	
Male, number/%	19/76.0%	11/78.6%	0.86
Age (years)	61±10 (45-81)	63±8 (52-80)	0.91
Mean ± SD (range)			
Tumor size (cm)	5.6±3.4 (2.5-10.0)	5.9±3.2 (3.0-11)	0.43
Mean ± SD (range)			
ISUP nucleolar grade			0.97
1/2	7	4	
3/4	18	10	
Pathological stage			0.46
T1	3	1	
T2	5	6	
T3	15	7	
Tumor necrosis	19/76.0%	11/79%	1.0
Number/%			
Extent of tumor necrosis	23±18% (5-60)	32±20% (5-60)	0.03
Mean ± SD (range)			
Pericellular fibrosis	5/20%	14/100%	0.000
Number/%			
Vasculopathy in small/medium vessels	10/40%	11/78.6%	0.02
Number/%			

grade and pathological stage (pT). Patients in the study group was treated with 2-7 cycles of sunitinib on a 4/2 schedule (50mg/day for 28 days followed by 14-day rest before the next cycle started).

Pathological examination of nephrectomy specimens

Surgical specimens were examined according to the College of American Pathologists cancer protocols (www.cap.org). Briefly, nephrectomy specimens were bivalved to reveal the tumors. Surgical margins, tumor size, anatomic extent of the tumor (perinephric and sinus invasion and vascular invasion), and percentage of tumor necrosis were documented. Tumors were sampled at 1 section/cm tumor for routine histological examination.

Immunohistomical staining and evaluation

Immunohistochical staining procedure followed the established protocol. One representative block from each case was stained for: CD34 (0.8 µg/ml, Ventana, Tucson, AZ), CA9 (1:2000, Novus Biologicals, Littleton, CO), and VEGFR2

(1:150, Cell Signaling, Danvers, MA). The 5-µm tissue sections were antgen-retrieved according to the specifications of the manufacturers of primary antibodies. The slides were then incubated sequentially with primary antibodies, biotinylated secondary antbody, avidin-peroxidase complex (Ventana, Tucson, AZ) and chromogenic substrate diaminobenzidine. The stains were performed on a Ventana Benchma-rk automatic stainer (Ventana, Tucson, AZ). The expression of CAIX was evaluated using a composite score which was calculated by multiplying the staining intensity (negative [0], week [1] and strong [2]) and percentages of positive cells (0-100). Therefore, the CAIX staining score ranged from 0 to 200.

Morphometric analysis of tumor microvessels

Evaluation of tumor microvessel density (MVD) and morphology was performed on CD34 immunostain slides. Representative tumor sections immunostained with CD34 were scanned at low magnification to identified five 4X fields with greatest number of tumor microvessels. For MVD, any discrete CD34-positive structure was counted as a tumor microvessel. Any contiguous structure, regardless of its branching contour, was counted as a microvessel. MVD was calculated as the number of microvessels per 4X field.

Tumor microvessels were also evaluated for their morphological alterations, including dilatation and fragmentation. In untreated tumors, tumor microvessels usually formed delicate and arborizing vasculature without conspicuous lumens (**Figure 1A**). In treated tumors,
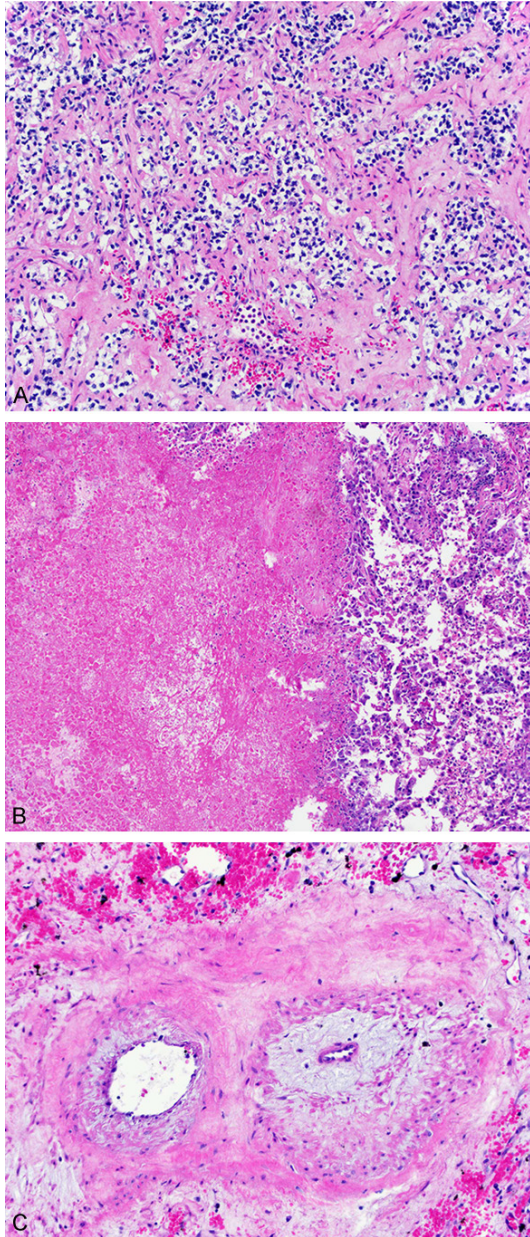
Figure 2. Morphological alterations in treated clear cell renal cell carcinoma include pericellular fibrosis (A), necrosis (B), and vasculopathy involving small and medium vessels with intimal thickening, myxoid change involving intima and media and luminal narrowing and occlusion (C).

tumor microvessels, however, often became dilated and discontinuous (**Figure 1C**). Tumor microvessel dilatation was categorized as normal (<10% microvessels showing dilation, **Figure 1A**), focal (10-50% microvessels showing dilation, **Figure 1B**) and diffuse (>50% microvessels showing dilation, **Figure 1C**). Similarly tumor microvessel fragmentation was catego-

rized as normal (≥90% microvessels forming arborizing vascular network with <10% short vessels, **Figure 1A**), focal (50-90% microvessels forming arborizing vascular network with 10-49% short vessels, **Figure 1B**) and diffuse (<50% microvessels forming arborizing vascular network with >50% short vessels, **Figure 1C**).

To evaluate the expression of VEGFR-2 on tumor microvessels, VEGFR-2 positive microvessels were counted in the same fashion as MVD was counted. Expression of VEGFR-2 was calculated as VEGFR-2/CD34 ratio.

Statistical analysis

Student t test was used for continuous variables and x^2 test was used for categorical variables. Statistical significance was set at p<0.05.

Results

There is no significant difference between the treated and control tumors in terms of gender distribution, age, tumor size, ISUP nucleolar grade and pathological stage (**Table 1**). The % of tumors with tumor necrosis (**Figure 2A**, **Table 1**) was not different between two groups. However, the treated tumors showed a significant increase in the amount of tumor necrosis compared with the untreated tumors (32% vs 23%, p=0.03, **Table 1**). Apoptosis was not significantly identified in both groups. Pericellular fibrosis, in which tumor cells were surrounded by hyalinized fibrous tissue (**Figure 2A**), was seen in all 14 treated tumors. Tumor cells with pericellular fibrosis had degenerative appearance with single cells and poorly formed nests with pyknotic nuclei separated by fibrous tissue with inconspicuous vascular septa (**Figure 2A**). Coagulative necrosis was seen in 11/14 (79%) of treated tumors (**Figure 2B**). These changes were interspersed within the tumor areas with no obvious treatment effect. Pericellular fibrosis was also seen, but in much lesser extent, in untreated tumors (5/20%, p<0.001, **Table 1**). There were small and medium vessels with intimal thickening and myxoid and hyalinized changes involving intima and media and resulting in luminal narrowing and occlusion (**Figure 2C**). Such changes were more common in treated tumors (11/78.6%) than untreated tumors (10/40%, p=0.02, **Table 1**).

Table 2. Morphological analysis of tumor microvessels in clear cell renal cell carcinomas

Morphological analysis	Untreated	Treated	P value
MVD	64	33	0.003
Number/4X fields			
Dilatation			0.004
Normal	7	0	
Focal	15	6	
Diffuse	3	8	
Fragmentation			0.014
Normal	12	0	
Focal	1	2	
Diffuse	12	12	
VEGFR2 expression	0.81±0.35	0.95±0.25	0.04
VEGFR2/CD34 ratio ± SD			

Treated tumors showed significantly reduced MVD (33/4X field) compared with untreated tumors (64/4X field, p=0.003, **Table 2**). The morphology of the tumor microvessels was also significantly different between treated and untreated tumors. Focal and diffuse vascular dilatation was observed in 6/14 and 8/14 treated tumors, and in 15/25 and 3/25 untreated tumors (p=0.004), while focal and diffuse vascular fragmentation was observed in 1/14 and 12/14 treated tumors, and 1/25 and 12/25 untreated tumors (p=0.014).

VEGFR-2 immunostain was found on the endothelial cells but not on tumor cells (**Figure 3A** and **3C**). The expression of VEGFR-2 on tumor microvessels was normalized against the CD-34 positive microvessels. VEGFR-2/CD34 ratio was higher in treated tumors (0.95) than untreated tumors (0.81, p=0.04).

Finally, CAIX immunostain was localized on tumor cell membranes. The composite staining score was 129.3±42.5 and 91.5±41.5 in untreated and treated tumors (p=0.09).

Discussion

The anti-tumor mechanisms of sunitinib in ccRCC have been previously studied using cell culture and mouse xenograft models and it is thought that sunitinib primarily targets the tumor angiogenesis rather than exerting direct effect on tumor cells. Histological examination of treated tumors is critical as it allows researchers to examine whether sunitinib targets the intended tissue and the effectiveness of treatment. It may also identify morphological features and tissue tumor markers that may correlate with the treatment response. Only two studies so far investigated the treatment effect in surgically resected ccRCC specimens [14, 17]. However, neither study provided a quantitative measurement of the treatment effect. In this study, we conducted a detailed analysis of both quantitative and qualitative alterations in tumor microvessels in surgically resected ccRCCs treated with sunitinib.

Our study confirmed that subinitib primarily affected tumor microvessels. The treated tumors showed almost 50% reduction in tumor microvessels (MVD= 33 in treated tumors vs 64 in untreated tumors), which resulted probably from both suppresson of neo-angiogenesis and destruction of preexisting tumor microvessels [19]. In addition, sunitinib treatment produced significant structural alterations in tumor microvessels. Microvascular dilatation and fragmentation were seen in all the treated tumors. The latter indicated highly tortuous microvascular network that appeared fragmented and discontinuous on tissue sections. Structural disruption of microvessels results in loss of physiological integrity of vessels leading to vessel leakage as evidenced by deposition of fibrinoid material and fibrosis in pericellular and sinosoidal pattern. The vasculopathy involving small and medium vessels with intimal and medial thickening and myxoid and hyalinized changes and luminal narrowing and occlusion, first reported by Tsuzuki et al. [18], is also seen in almost 80% of treated tumors. The reduction in MVD and structural alterations seen in tumor vessels result in increased extent of necrosis in treated tumors which was increased by almost 40% (from 23% in untreated tumors to 32% in treated tumors) even though both treated and untreated tumors did not differ significantly in tumor size, stage and nuclear grade.

However, the structural disruption, including microvascular dilatation and fragmentation, vasculopathy involving small and medium vessels and pericellular fibrosis were also found in untreated tumors, although these changes were significantly less common and severe in untreated tumors. These findings suggest the
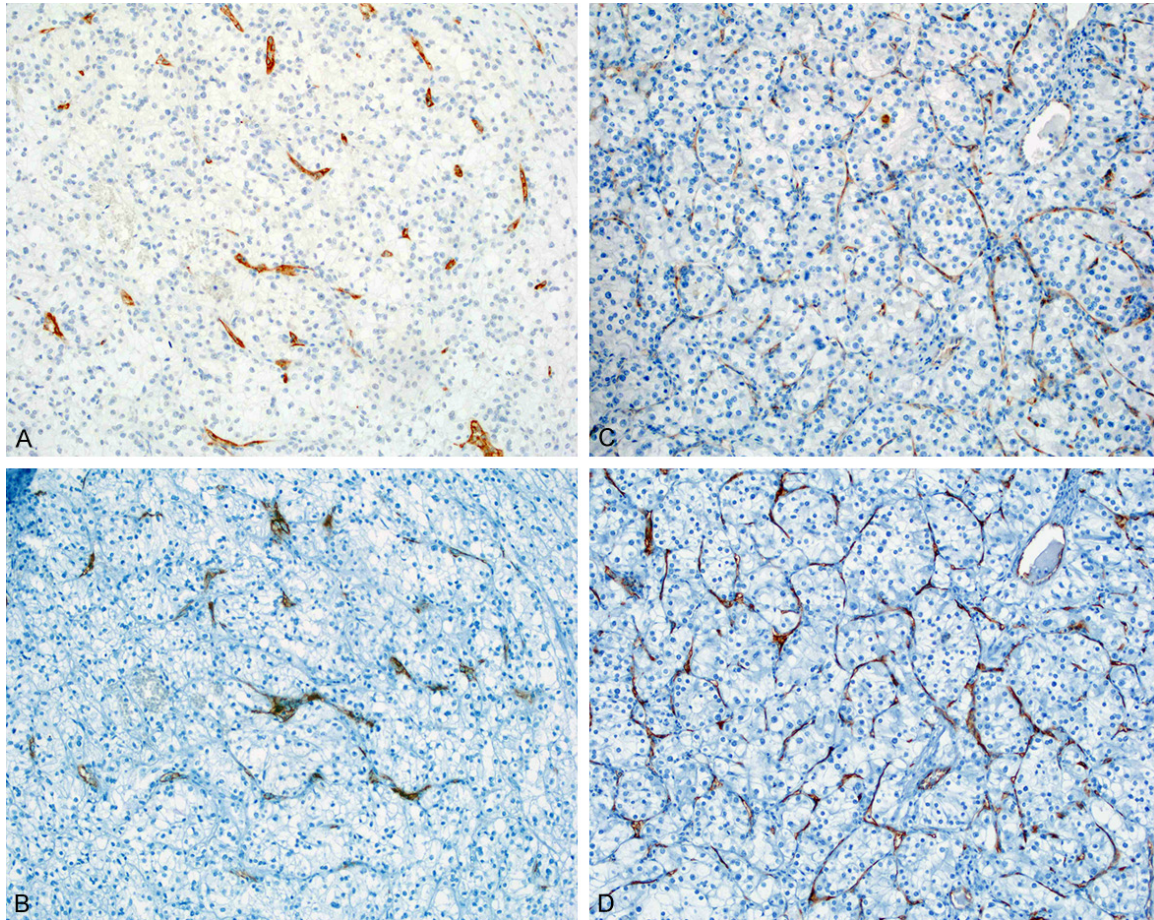
Figure 3. Expression of VEGFR-2 on tumor microvessels in treated (A) and untreated (C) tumors. CD34 immunostains highlighted microvessels in treated (B) and untreated (D) tumors.

architectural changes in tumor vessels are not specific for sunitinib treatment. The tumor vessels are inherently architecturally unstable and prone to structural alterations such as dilatation, fragmentation and tortuosity. Sunitinib, however, augments these changes, presumably by increasing the endothelial permeability and loss of pericytes [14, 19] and therefore modulating the structure and function of tumor microvessels and consequently exerting its anti-tumor effect.

Another important finding of this study is that the treated tumors had higher expression of VEGFR-2 (VEGFR-2/CD34 ratio) on tumor microvessels which were significantly reduced in number. The mechanism by which sunitinib increased the VEGFR-2 expression on the residual tumor microvessels was not studied in this report but it is possible that hypoxia and ischemia resulting from sunitinib treatment may up-regulate VEGFR-2 expression on residu-

al tumor microvessels. This finding may have important therapeutic implications. Sunitinib is a multi-kinase inhibitor that targets VEGFR-2 which plays a critical role in angiogenesis. Although treatment with sunitinib substantially improves patient outcome, the initial success is overshadowed by the occurrence of resistance. The mechanisms of resistance are poorly understood [20], but increased expression of VEGFR-2 on tumor vessels could play a role in the development of the resistance. Therefore, further, more specific inhibition of VEGFR-2 may help overcome the resistance in treated ccRCC. A recent study by Duignan et al. [15] using a more specific anti-VEGFR-2 antibody DC101 found that combined use of sunitinib and DC101 reduced the tumor volume to an extent greater than with sunitinib or DC101 used alone in a murine RCC model.

In summary, we conducted a detailed morphological analysis of the sunitinib treatment effect

in surgically resected ccRCC specimens. Our study shows that the tumor microvessels are the primary target of sunitinib treatment in ccRCC. Sunitinib treatment significantly reduces the microvessel density and also produces significant structural alterations that lead to hypoxia and ischemia and necrosis in tumors. The treatment also increases the VEGFR-2 expression on the residual tumor microvessels and may contribute to the occurrence of resistance to sunitinib treatment.

Disclosure of conflict of interest

None.

Address correspondence to: Dr. Ming Zhou, Departments of Pathology and Urology, New York University Langone Medical Center, New York, USA. Tel: 780-432-8338; Fax: 780-432-8214; E-mail: Ming.Zhou@nyumc.org

References

[1] Cohen D and Zhou M. Molecular genetics of familial renal cell carcinoma syndromes. Clin Lab Med 2005; 25: 259-277.

[2] Gossage L, Eisen T and Maher ER. VHL, the story of a tumour suppressor gene. Nat Rev Cancer 2015; 15: 55-64.

[3] Rini BI, Campbell SC and Escudier B. Renal cell carcinoma. Lancet 2009; 373: 1119-1132.

[4] Cancer Genome Atlas Research Network. Comprehensive molecular characterization of clear cell renal cell carcinoma. Nature 2013; 499: 43-49.

[5] Dalgliesh GL, Furge K, Greenman C, Chen L, Bignell G, Butler A, Davies H, Edkins S, Hardy C, Latimer C, Teague J, Andrews J, Barthorpe S, Beare D, Buck G, Campbell PJ, Forbes S, Jia M, Jones D, Knott H, Kok CY, Lau KW, Leroy C, Lin ML, McBride DJ, Maddison M, Maguire S, McLay K, Menzies A, Mironenko T, Mulderrig L, Mudie L, O'Meara S, Pleasance E, Rajasingham A, Shepherd R, Smith R, Stebbings L, Stephens P, Tang G, Tarpey PS, Turrell K, Dykema KJ, Khoo SK, Petillo D, Wondergem B, Anema J, Kahnoski RJ, Teh BT, Stratton MR and Futreal PA. Systematic sequencing of renal carcinoma reveals inactivation of histone modifying genes. Nature 2010; 463: 360-363.

[6] Duns G, van den Berg E, van Duivenbode I, Osinga J, Hollema H, Hofstra RM and Kok K. Histone methyltransferase gene SETD2 is a novel tumor suppressor gene in clear cell renal cell carcinoma. Cancer Res 2010; 70: 4287-4291.

[7] Guo G, Gui Y, Gao S, Tang A, Hu X, Huang Y, Jia W, Li Z, He M, Sun L, Song P, Sun X, Zhao X, Yang S, Liang C, Wan S, Zhou F, Chen C, Zhu J, Li X, Jian M, Zhou L, Ye R, Huang P, Chen J, Jiang T, Liu X, Wang Y, Zou J, Jiang Z, Wu R, Wu S, Fan F, Zhang Z, Liu L, Yang R, Wu H, Yin W, Liu Y, Peng H, Jiang B, Feng Q, Li C, Xie J, Lu J, Kristiansen K, Li Y, Zhang X, Li S, Wang J, Yang H and Cai Z. Frequent mutations of genes encoding ubiquitin-mediated proteolysis pathway components in clear cell renal cell carcinoma. Nat Genet 2012; 44: 17-19.

[8] Pena-Llopis S, Vega-Rubin-de-Celis S, Liao A, Leng N, Pavia-Jimenez A, Wang S, Yamasaki T, Zhrebker L, Sivanand S, Spence P, Kinch L, Hambuch T, Jain S, Lotan Y, Margulis V, Sagalowsky AI, Summerour PB, Kabbani W, Wong SW, Grishin N, Laurent M, Xie XJ, Haudenschild CD, Ross MT, Bentley DR, Kapur P and Brugarolas J. BAP1 loss defines a new class of renal cell carcinoma. Nat Genet 2012; 44: 751-759.

[9] Varela I, Tarpey P, Raine K, Huang D, Ong CK, Stephens P, Davies H, Jones D, Lin ML, Teague J, Bignell G, Butler A, Cho J, Dalgliesh GL, Galappaththige D, Greenman C, Hardy C, Jia M, Latimer C, Lau KW, Marshall J, McLaren S, Menzies A, Mudie L, Stebbings L, Largaespada DA, Wessels LF, Richard S, Kahnoski RJ, Anema J, Tuveson DA, Perez-Mancera PA, Mustonen V, Fischer A, Adams DJ, Rust A, Chan-on W, Subimerb C, Dykema K, Furge K, Campbell PJ, Teh BT, Stratton MR and Futreal PA. Exome sequencing identifies frequent mutation of the SWI/SNF complex gene PBRM1 in renal carcinoma. Nature 2011; 469: 539-542.

[10] Gnarra JR, Tory K, Weng Y, Schmidt L, Wei MH, Li H, Latif F, Liu S, Chen F, Duh FM, et al. Mutations of the VHL tumour suppressor gene in renal carcinoma. Nat Genet 1994; 7: 85-90.

[11] Baldewijns MM, van Vlodrop IJ, Vermeulen PB, Soetekouw PM, van Engeland M and de Bruine AP. VHL and HIF signalling in renal cell carcinogenesis. J Pathol 2010; 221: 125-138.

[12] Na X, Wu G, Ryan CK, Schoen SR, di'Santagnese PA and Messing EM. Overproduction of vascular endothelial growth factor related to von Hippel-Lindau tumor suppressor gene mutations and hypoxia-inducible factor-1 alpha expression in renal cell carcinomas. J Urol 2003; 170: 588-592.

[13] Ljungberg B, Bensalah K, Canfield S, Dabestani S, Hofmann F, Hora M, Kuczyk MA, Lam T, Marconi L, Merseburger AS, Mulders P, Powles T, Staehler M, Volpe A and Bex A. EAU guidelines on renal cell carcinoma: 2014 update. Eur Urol 2015; 67: 913-924.

[14] Huang D, Ding Y, Li Y, Luo WM, Zhang ZF, Snider J, Vandenbeldt K, Qian CN and Teh BT. Sunitinib acts primarily on tumor endothelium rather than tumor cells to inhibit the growth of

renal cell carcinoma. Cancer Res 2010; 70: 1053-1062.

[15] Duignan IJ, Corcoran E, Pennello A, Plym MJ, Amatulli M, Claros N, Iacolina M, Youssoufian H, Witte L, Samakoglu S, Schwartz J, Surguladze D and Tonra JR. Pleiotropic stromal effects of vascular endothelial growth factor receptor 2 antibody therapy in renal cell carcinoma models. Neoplasia 2011; 13: 49-59.

[16] Smith NR, Baker D, Farren M, Pommier A, Swann R, Wang X, Mistry S, McDaid K, Kendrew J, Womack C, Wedge SR and Barry ST. Tumor stromal architecture can define the intrinsic tumor response to VEGF-targeted therapy. Clin Cancer Res 2013; 19: 6943-6956.

[17] Sharpe K, Stewart GD, Mackay A, Van Neste C, Rofe C, Berney D, Kayani I, Bex A, Wan E, O'Mahony FC, O'Donnell M, Chowdhury S, Doshi R, Ho-Yen C, Gerlinger M, Baker D, Smith N, Davies B, Sahdev A, Boleti E, De Meyer T, Van Criekinge W, Beltran L, Lu YJ, Harrison DJ, Reynolds AR and Powles T. The effect of VEGF-targeted therapy on biomarker expression in sequential tissue from patients with metastatic clear cell renal cancer. Clin Cancer Res 2013; 19: 6924-6934.

[18] Tsuzuki T, Sassa N, Shimoyama Y, Morikawa T, Shiroki R, Kuroda M, Fukatsu A, Kuwahara K, Yoshino Y, Hattori R and Gotoh M. Tyrosine kinase inhibitor-induced vasculopathy in clear cell renal cell carcinoma: an unrecognized antitumour mechanism. Histopathology 2014; 64: 484-493.

[19] Faivre S, Demetri G, Sargent W and Raymond E. Molecular basis for sunitinib efficacy and future clinical development. Nat Rev Drug Discov 2007; 6: 734-745.

[20] Joosten SC, Hamming L, Soetekouw PM, Aarts MJ, Veeck J, van Engeland M and Tjan-Heijnen VC. Resistance to sunitinib in renal cell carcinoma: From molecular mechanisms to predictive markers and future perspectives. Biochim Biophys Acta 2015; 1855: 1-16.